

## Accepted Manuscript

Title: Molecular dynamics simulations to calculate glass transition temperature and elastic constants of novel polyethers

Author: Radhakrishnan Sarangapani Sreekantha T. Reddy  
Arun K. Sikder



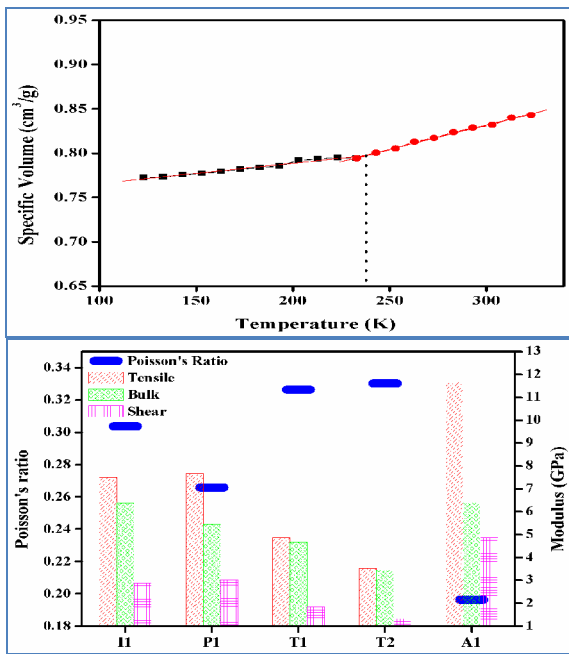
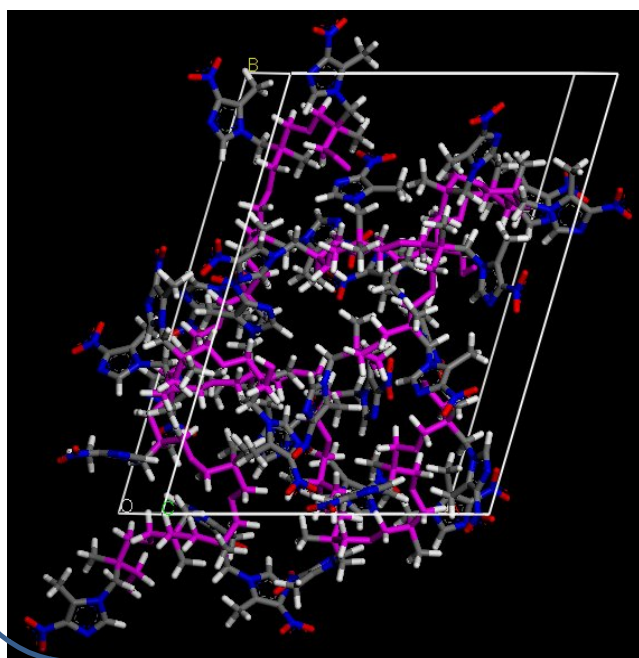
PII: S1093-3263(15)00030-3  
DOI: <http://dx.doi.org/doi:10.1016/j.jmgm.2015.01.011>  
Reference: JMG 6512

To appear in: *Journal of Molecular Graphics and Modelling*

Received date: 18-8-2014  
Revised date: 28-1-2015  
Accepted date: 29-1-2015

Please cite this article as: R. Sarangapani, S.T. Reddy, A.K. Sikder, Molecular dynamics simulations to calculate glass transition temperature and elastic constants of novel polyethers, *Journal of Molecular Graphics and Modelling* (2015), <http://dx.doi.org/10.1016/j.jmgm.2015.01.011>

This is a PDF file of an unedited manuscript that has been accepted for publication. As a service to our customers we are providing this early version of the manuscript. The manuscript will undergo copyediting, typesetting, and review of the resulting proof before it is published in its final form. Please note that during the production process errors may be discovered which could affect the content, and all legal disclaimers that apply to the journal pertain.



**Highlights of the study:**

1. Hydroxyl terminated polyethers functionalized with nitrogen heterocycles derived from novel oxetane monomers are studied by atomistic simulations
2. Most probable configuration of polymer models (Equilibrium structure) have been derived by the series of MD simulations under NVT and NPT ensembles
3. Glass transition temperature ( $T_g$ ) is calculated from its equilibrium structure by further series of NPT-MD calculations using an annealing protocol. Plot of specific volume as a function of temperature is used for the determination of  $T_g$ .
4. Elastic tensors and mechanical properties of polymer models are predicted from the NPT-MD simulations. Parrinello method is employed for studying the stress-strain relationship.
5. Polymers with triazole and imidazole derivatives possess relatively better mechanical properties compared to others and predicted explosive performance revealed that pyrazole derivatives are superior in terms of performance while the triazole and tetrazole derivatives are predicted to exhibit moderate performance.

## Molecular dynamics simulations to calculate glass transition temperature and elastic constants of novel polyethers

Radhakrishnan Sarangapani<sup>a,\*</sup>, Sreekantha T. Reddy<sup>b</sup>, Arun K. Sikder<sup>a</sup>

<sup>a</sup> High Energy Materials Research Laboratory, Pune-411 021, India

<sup>b</sup> Defence Metallurgical Research Laboratory, Hyderabad-500 058, India

### Abstract

Molecular dynamics simulations studies are carried out on hydroxyl terminated polyethers that are useful in energetic polymeric binder applications. Energetic polymers derived from oxetanes with heterocyclic side chains with different energetic substituents are designed and simulated under the ensembles of constant particle number, pressure, temperature (NPT) and constant particle number, volume, temperature (NVT). Specific volume of different amorphous polymeric models is predicted using NPT-MD simulations as a function of temperature. Plots of specific volume versus temperature exhibited a characteristic change in slope when amorphous systems change from glassy to rubbery state. Several material properties such as Young's, shear, and bulk modulus, poisson's ratio, etc are predicted from equilibrated structures and established the structure-property relations among designed polymers. Energetic performance parameters of these polymers are calculated and results reveal that the performance of the designed polymers is comparable to the bench-mark energetic polymers like polyNIMMO, polyAMMO and polyBAMO. Overall, it is worthy remark that this molecular simulations study on novel energetic polyethers provides a good guidance on mastering the design principles and allows us to design novel polymers of tailored properties.

**Keywords:** Molecular dynamics, Energetic polymers, Glass transition temperature, Elastic properties, Energetic performance

## 1. Introduction

Energetic polymers with excellent mechanical properties are being demanded for their use as binder in high performance propellant applications. These polymers are widely applied in polymer bonded explosives (PBX) and propellants to improve mechanical properties of mixture, good safety, to reduce brittleness of explosive, and to increase strain capability [1-4]. Attempts were made to replace hydroxyl-terminated polybutadiene (HTPB) binder to achieve the superior performance by energetic polymer systems comprising of glycidyl azide polymer (GAP) and bis(azidomethyl) oxetane (BAMO) copolymers as polymer matrix in combination with plasticizers [5]. In addition, superior combustion properties were also observed for HMX propellant with BAMO and nitratomethyl methyl oxetane (NIMMO) binder and BAMO-NIMMO co-polymer are preferred to improve shock sensitivity characteristics [5]. The selection of the polymer possessing high strength and good adhesive with the benchmark explosives is also a key parameter. It is time-consuming to obtain the formulation by many tests for mechanical and interface properties and the process lacks safety [6-9]. As a result, there are many calculations and simulation studies used to understand interactions between polymer chains and explosives with quantum mechanics (QM), molecular mechanics (MM) and molecular dynamics (MD) methods [10-16]. Recently, Cho et al [17], reported the limits of superheating of water and supercooling of vapor from Monte Carlo simulations using microscopic models with configurational enthalpy as the order parameter. They used generalized replica exchange method (GREM) and performed umbrella sampling for a number of enthalpy windows and well reproduced the superheating limits. An approach for directly determining the liquid-vapor phase equilibrium of a model system at any temperature along the coexistence line is described by Jeffrey and the method relies on transition matrix Monte Carlo concepts. This method provided very precise estimates of liquid-vapor phase coexistence properties in a reasonable amount of CPU time [18]. Molecular dynamics simulations were also interestingly used to study the phase transition and mechanical properties of a high explosive, HMX under different temperatures and pressures by Cui et al [19]. In our previous work, we discussed quantum-chemical design and screening of various novel energetic oxetanes, which usually construct the backbone for these energetic polymers [20]. The approach is used to improve energy content of polymer by the insertion of variousazole derivatives. This extended study investigates the polymers of those model compounds by using atomistic simulations.

In rocket propellant applications, polymer primarily binds one or more energetic solids in a plastic matrix, aids in processing and mechanically holds all the ingredients together,

serving as a structural element. Hence, prediction of mechanical and structural behavior of the binders is vital. Recent years, molecular modeling techniques based on classical molecular mechanics have become promising methods for the investigation of structural, thermodynamic and mechanical properties of amorphous polymers [21-23]. In general, the stress in the solid (or a group of interacting particles in the form of solid) is defined as change in the internal energy per unit volume with respect to the strain. The stiffness co-efficient can be obtained by estimating the second derivatives of potential energy with respect to strain. In principle, mechanical properties of a material can be derived from its elastic co-efficient matrix. There are 21 independent elastic coefficients but material symmetries further reduce the number of independent elastic coefficients. For an isotropic substance there are only two independent elastic coefficients namely Lamé coefficients based on which Young's, Shear and bulk modulus and Poisson's ratio can be attained (details are given in Supporting Information) [24,25]. The hardness, tensile strength, fracture strength and elongation in tension, can be related to the elastic moduli. Hardness and tensile strength representing the resistance to plastic deformation are proportional to the shear modulus  $G$ . Fracture strength is proportional to the bulk modulus  $K$ . The quotient  $K/G$  indicates the extent of the plastic range, so that a high value of  $K/G$  is associated with ductility and a low value with brittleness. Extensive studies were carried out on PBX in order to understand physical, chemical and mechanical behavior of the constituents of PBX formulations as well as the interactions between them from the MD simulations. Xiao et al. studied various energetic materials like triamino trinitro benzene (TATB), bicyclo-HMX, CL-20 etc. with fluorine containing polymers [26-28] and employed the classical mechanics to predict elastic constants. Li et al. investigated effect of azidomethyl methyl oxetane (AMMO) on different crystalline surfaces of RDX and predicted that the mechanical properties of RDX can be effectively improved by adding some amounts of AMMO [29].

Molecular dynamics simulations were successfully applied to determine glass transition temperature ( $T_g$ ) for amorphous polymers.  $T_g$  can be estimated based on the change in thermal expansion co-efficients in ensembles held at constant pressure and temperature [30] or the change in the temperature dependence of diffusivity of atoms in ensembles held at constant volume and temperature [31]. Bermejo et al demonstrated the prediction of glass transition temperatures of pure and cross-linked Poly vinyl acetates by atomistic modeling [21].

The present investigation aims to model hydroxyl terminated energetic polyethers based on novel oxetane monomers functionalized with nitrogen heterocycles. Density, mechanical properties, and glass transition temperature of these polymers are simulated using molecular

dynamics and energetic performance of these polymers is calculated by empirical methods. Structure-property relationships are established that brings basic insight on the effect of molecular structure over macro properties and also guide to master the design principles. Comprehensive analysis of simulated quantities and calculated energetic performance identify the candidate polymers for rocket propellant applications.

## 2. Computational Method

Chemical structures of repeating units of polymers are shown in Fig. 1. Molecular dynamics simulations are carried out in Discover and Amorphous cell Suites of Materials Studio 4.3, Accelrys Inc. A well validated condensed-phase optimized molecular potentials for atomistic simulation studies (COMPASS) force field is used for the simulation [32]. It is an *ab initio* force field that enables accurate and simultaneous prediction of gas-phase properties (structural, conformational, vibrational, etc.) and condensed-phase properties (equation of state, cohesive energies, etc.) for a broad range of molecules and polymers. COMPASS is parameterized in two phases: *ab initio* parameterization and empirical optimization. In the first phase, partial charges and valence parameters were derived by fitting to *ab initio* potential energy surfaces and the van der Waals parameters were fixed to a set of initial approximated parameters. In the second phase, emphasis was on optimizing the force field to yield good agreement with experimental data. The parameters for covalent molecules are well validated using various calculation methods including extensive MD simulations of liquids, crystals, and polymers. Previous studies on energetic materials confirmed its applicability to nitramines [13,27] and hence COMPASS is chosen for this investigation. The initial configurations are generated in several steps. Amorphous builder is used to construct a cell containing 3 chains that are terminated with hydroxyl group, each containing 10 monomeric units (Degree of polymerization,  $D_p=10$ ). Thus, in order to avoid surface effects, 3D periodic boundary conditions are used. In all the condensed phase simulation cases, electrostatic interactions are treated using the group based summation, non-bonded interactions are truncated at 12.50 Å, the Verlet velocity integration method is used with a time step of 1fs.

The constructed cells are subjected to equilibration consisting of various steps. Initially the energy of generated amorphous cell is minimized to convergence value of 0.001 kcal/mol/Å. In order to bring the polymer model system to the most probable configuration consistent with target temperature and pressure, cell relaxations are performed for the energy minimized cells of polymer models using NVT-MD simulations. The relaxation protocol

employed is similar to the Hoffmann's relaxation protocol (details are given in Supporting Information) [33]. Karayiannis et. al. [23] modified the above protocol to perform NPT dynamics at the end of the NVT cycles. Berendsen method is used for temperature and pressure control. The final structure has been taken from the relaxation simulation and it is equilibrated by NPT-MD simulations for 250ps (production run). The specific volume and energy was observed to fluctuate about a well-defined mean over the time scale of dynamics, indicating that the equilibrium density and energy for the given temperature and pressure has been attained and the system is in the most probable configuration.

In order to predict the glass transition temperature, the equilibrium structure from the above simulation is subjected to further series of dynamics in ensembles held at constant particle number, pressure and temperature. An annealing protocol at high temperature was followed, the temperature was dropped from 323K by a fixed amount ( $\Delta T=10K$ ), under atmospheric pressure using NPT ensemble. After careful selection the cooling rate of 10K/200 ps is used. It is controlled by the Berendsen thermostat and the pressure by the Berendsen barostat. Each subsequent dynamic step started with the structure and velocities from previous temperature. This step is repeated until the annealing temperature is well below  $T_g$  of designed polymers. Plot of specific volume as a function of temperature is used for the determination of glass transition temperature. The observed change in the slope is related to  $T_g$  of these systems corresponding to a transition between a glassy state, where molecules are frozen in place to a rubbery state, where molecules can start to wiggle around. Molecular dynamics simulations have been successfully applied to predict elastic tensors and mechanical properties of different type of polymers. In contrast to the prediction protocol of  $T_g$ , Parrinello and Anderson methods are used for pressure and temperature control during NPT-MD simulation for 250ps (production run). Parrinello method is useful for studying the stress-strain relationship in materials and it is allowed to change both shape and volume of the cell, so that internal stress of the system can match the externally applied stress. The elastic tensors and mechanical properties are estimated by the static mechanics as implemented in the Materials Studio Suite.

The performance of an energetic compound is a function of its density, oxygen balance, and heat of formation. The calculations of detonation velocity ( $D$ , in km/s) and detonation pressure ( $P$ , in GPa) are performed by using the Kamlet-Jacobs equations [34,35] as follows:

$$D = 1.01(NM^{1/2}Q^{1/2})^{1/2}(1 + 1.30\rho) \text{ and } P = 1.55\rho^2 NM^{1/2}Q^{1/2}$$



In the above equations,  $N$  is moles of gaseous detonation products per gram of explosives,  $M$  is average molecular weights of gaseous products,  $Q$  is chemical energy of detonation (cal/g) defined as the difference of the HOFs between products and reactants, and  $\rho$  is the density of explosive ( $\text{g}/\text{cm}^3$ ). We assumed  $\text{N}_2$ ,  $\text{H}_2\text{O}$ ,  $\text{CO}_2$  and  $\text{C}$  (s) as important detonation products, explained by Kamlet et al [34,35] and Politzer et al [36] for CHNO based energetic compounds using  $\text{H}_2\text{O}$ - $\text{CO}_2$  arbitrary decomposition scheme.

### 3. Results and Discussion

The ability to predict the properties from the chemical constitution of chains is critical in the, design and development of new polymer products in an industrial point of view. Atomistic molecular modeling simulations on pure amorphous models of the various molecules under investigation have been performed. Amorphous phase is built under periodic boundary conditions, and a model with low potential energy is obtained and used for further investigation. Representative model of well relaxed Poly**I4** is shown given in Fig. 2.

#### 3.1. Density

Densities varied during NPT dynamics simulations, and the system was allowed to evolve until the average density remained constant (Fig. 3). Final densities of designed polymer molecules are given in Table I. Density of the substituted polyethers is ranging from 0.6 to 1.4 g/cc. Polymers containing azetidine side chain are possessing poor density while polymers with pyrazole side chain have higher density. Analysis of density data of various imidazole derivatives clearly reveals that introduction of one nitro group increases the density while the further introduction of nitro group (**I5**) does not significantly alter the density. Comparison of polymers **I2** and **I3** shows that position of nitro group does not allow much variation in packing and hence have almost identical density. Similar to imidazole side chains, introduction of nitro group increases density in pyrazole side chains also. It is reported that  $\text{CF}_3$  group increases the density, which is seen in the present study also. Comparison of **P1**, **P3** and **P4** reveals an increase in density from 1.145 to 1.377 g/cc. Difluoro pyrazole chain (**P4**) is observed to be high dense polymer among the studied compounds. In case of triazole side chains, isomeric triazole rings (**T1** and **T2**) possess similar density, while increase in density is also observed in nitro triazole (**T3**) side chain like in earlier cases. Tetrazole side chain based polyethers are possessing moderate density of about 1.2 g/cc while azetidine derivatives possess low density of about 0.7 g/cc. This may be attributed to the

strain induced from the azetidine ring to the back bone. Comparison of **I1** & **P1** and **T1** & **T2** sets clearly tells about the role of positional isomers on polymer densities. Presence of adjacent nitrogen brings better packing than the other (**I1**). Densities of well-known/benchmark energetic binders viz., poly NIMMO, poly AMMO and poly BAMO are also calculated at the same level of theory and found to be comparable with experimental results. This confirms the validity of theoretical methodology.

### 3.2. Glass transition temperature

The glass transition temperature is probably one of the most important properties of polymers because it determines the processing and working temperature range. A number of different methods have been used to identify the  $T_g$  of polymers in molecular-dynamics simulations [37]. One commonly used approach is to study the change in density or specific volume as a function of temperature in ensembles held at constant particle number, pressure and temperature. In order to study the glass transition of designed polymers an annealing protocol at high temperature was followed. The change of specific volume as a function of temperature is plotted for the designed polymers. It is clear for all the systems that specific volume decreases with decreasing temperature and a change in the slope is observed. This is due to different linear relationship between specific volume and temperature at below and above the glass transition temperature. Above the glass transition (rubbery phase) the specific volume will decrease more rapidly with decreasing temperature than in the glassy phase and this phenomenon of a change in slope is used for determining  $T_g$ . Representative graph of specific volume versus temperature data of PolyAMMO is shown in Fig. 4. Table II compiles the predicted glass transition temperature data of various designed polymers along with bench-mark energetic polymers (polyNIMMO, polyAMMO and polyBAMO). Simulated glass transition temperature of polyNIMMO and polyAMMO matches well with experimental data [38-40]. This shows the validity of simulation methodology. Simulated glass transition temperature of unsubstituted heterocyclic side chains is shown Fig. 5. The more flexible the backbone chain is, the lower its  $T_g$  will be and this will facilitate the low temperature properties of polymer. In the present study the backbone flexibility decreases in the following order **T2**>**T1**>**I1**=**A1**~**P1** and  $T_g$  in reverse order. This clearly reveals that azetidine side chain in the polyether backbone possess more rigidity while triazole side chain offers flexibility to the back bone. Among the imidazole side chained poly ethers, **I4** that possess methyl and nitro substitution in the imidazole side chain possess lowest  $T_g$ . Comparison of **P4** and **I5** shows that disubstitution in side chain leads to increase rotation barrier and hence relatively

higher  $T_g$  than their respective mono substitution. Role of structural isomerism on  $T_g$  can be realized on analyzing the data of **I2**, **I3** and **T1**, **T2** pairs. Nitro group at 4<sup>th</sup> position of imidazole side chain (**I2**) offers better mobility than at 2<sup>nd</sup> position (**I4**); while in the case of **T1** and **T2**, consecutive nitrogen in the triazole ring(**T2**) allows the sidechain to be away from the backbone and hence, exhibits lower  $T_g$  compared **T1**.

### 3.3. Mechanical properties

Mechanical properties are mainly due to the behavior exhibited by polymeric systems under different testing modes of elastics properties; each one defining a characteristic modulus [Youngs (E), Shear (G) and bulk (B)]. Recently, molecular dynamics simulations have been employed to predict these elastic properties. Mechanical properties calculation can be carried out using one of the static, dynamic or fluctuation formula approaches. However, dynamic and fluctuation methods have not been used frequently due to different reasons; for instance the long duration simulations required coupled to big uncertainties in its measurement and slow convergence of the elastic coefficients, respectively. Hence the static method is applied to calculate the mechanical properties. In this work, the mechanical properties of designed polymers are calculated using constant strain minimization method. In order to avoid any problem on the elastic property calculation, it is important to highlight that polymer system conformation are carefully selected from previous MD/minimization runs. It is required to have internal stress tensor components very close to zero ( $\leq 0.001$ ), which indicates a well relaxed/equilibrated configuration suitable for this type of calculation. The calculated stiffness matrices are checked for the isotropy condition, where-in non-diagonal components should be zero. However, for these systems diagonal components of this matrix are not zero but they are much higher than non-diagonal components. In addition, the matrix is symmetrical too. These are typical features of an amorphous isotropic system [41].

Table III shows the effective isotropic mechanical properties that include tensile/Young's modulus E, bulk modulus K, shear modulus G, and Poisson's ratio  $\gamma$  of various heterocycle functionalized poly ethers at 303K. All the moduli can be used to measure the extent of rigidity or stiffness of material, an indication of the capability of a material to resist the changes of shape or volume caused by external stress. Meanwhile, the resistance to plastic deformation is proportional to the shear modulus and the fracture strength is proportional to the bulk modulus. Larger the moduli, stiffer the material and smaller the deformation of the material is. Comparison of modulus data of designed polymers with the bench-mark energetic polymers like polyNIMMO, polyAMMO and polyBAMO reveals that

these designed polymers are stiffer and this is due to the rigidity introduced by the heterocyclic side chains. Fig. 6 shows that all three moduli are lower for polyethers having triazole side chains while azetidine polyethers possess very high values. This clearly reveals that triazole side chain brings plastic nature to the backbone and deform relatively better unlike others. While in the case of azetidine side chain inherent strain in the molecule bring rigidity to the chain and hence this polymer is simulated to be stiff. Relative order of susceptibility to deformation in these designed polymers within their group is shown in Table IV. This trend line grouping bring qualitative picture about the role of substitutions on the mechanical properties which is useful in relative ranking and screening of designed polymers for deemed applications. Introduction of nitro group in Imidazole side chained polyethers decreases the shear modulus (G) that confirms increase of plastic deformation nature. The similar behavior is also seen in case of pyrazole based polyethers while triazole side chain polymers do not follow this trend. Comprehensive analysis of modulus data of **I2**, **P2** and **T3** reveals the effect of mono nitro substitution in heterocycle side chain on modulus and this follows the increasing order of plasticity as **T3** < **I2** < **P2**. Comparison of moduli of polymers such as **P3**, **P4**, **I4** and **T5** indicates presence of alkyl or substituted alkyl groups imparts flexibility to the polymer.

The Poisson's ratio correlates various isotropic moduli through the formula  $E=3K(1-2\gamma)=2G(1+\gamma)$ , which can be used to evaluate the plasticity of the material. Comparison of the Poisson's ratio shows that all designed polymers possess superior plastic properties, since they have larger Poisson's ratio (about 0.3) except azetidine side chain polyethers. Fig. 6 reveals that predicted Poisson's ratio supports the modulus data. Polyethers having triazole side chain possess high Poisson's ratio while azetidine side chain possess very low value which confirms that plastic properties are better in triazole substituted polymers among them. The ratio of bulk modulus to shear modulus (K/G) can be used as an indication of the extent of the plastic range for a material. Generally, a larger value of K/G is associated with a better malleability of the materials [42]. PolyAMMO possess the best malleability while many of the designed polymers are comparable with polymers of NIMMO and BAMO. Overall, **I4**, **T1**, **T2** and **T4** exhibit relatively higher K/G values among the designed polymers. Polymers with triazole and imidazole derivatives possess relatively better mechanical properties compared to others.

Overall, this simulation study of predicting mechanical properties is useful in establishing structure-property relations and led the way to screening of designed polymers for deemed applications. Further, it should also be kept in mind that comparison with

experimental results is even difficult for pure polymers because it is well known that preparation conditions (solvent casting/hot press) play an important role on the formation of different percentages of amorphous/crystalline structure which are not well reproduced by MD simulations. In spite of that, it is worthy of remark that molecular simulations in principle provide a good estimation for strength of material under study since the model systems inherently lack of some details/defects which may be present in actual/real polymers.

### 3.4. Explosive performance

Table I lists the predicted detonation velocity ( $D$ ) and pressure ( $P$ ) of designed polyether derivatives. In case of imidazole containing polyethers, the calculated  $D$  is moderate; however, the  $D$  of dinitro derivative (**I5**) is comparable to AMMO and BAMO. This can be attributed to the relatively higher chemical energy of detonation ( $Q$ ) and density. In general, pyrazole derivatives are superior in terms of performance while the triazole and tetrazole derivatives are predicted to exhibit moderate performance ( $D = 4.3$  to  $5.6$  km/s and  $P = 5.9$  to  $11.2$  GPa). Fig. 7 represents the detonation velocity and pressure data of designed polymers compared with polyNIMMO, polyBAMO, and polyAMMO. Due to the low density, azetidine derivatives show poor performance. Similar to the velocity of detonation, detonation pressure also follows the above trend. Polymers of **I5**, **P2**, **P3**, **P4**, and **T3** are calculated to have detonation pressure higher than 10 GPa, which is relatively better than bench-mark energetic polymers.

## 4. Conclusions

Molecular dynamics simulations were carried out on hydroxyl terminated polyethers of novel oxetane monomers that are functionalized with nitrogen heterocycles to predict the structural, thermodynamic and mechanical properties of these amorphous polymers. Average densities of the designed polymers were achieved by performing NPT-MD calculations and density of the substituted polyethers is ranging from 0.6 to 1.4 g/cc. In order to study the glass transition of designed polymers, specific volume of different amorphous polymeric models was predicted using NPT-MD simulations as a function of temperature by adopting an annealing protocol at high temperature. The predicted glass transition temperature data of bench-mark energetic polymers (polyNIMMO, polyAMMO and polyBAMO) are well correlated with the experimental data. Analysis of the  $T_g$  data was useful in understanding the role of side-chain on  $T_g$ . Mechanical properties were predicted by simulating the equilibrated polymer models in NPT ensembles with Parrinello pressure control. The properties were

compared among the designed polymers and the relative order of susceptibility to deformation was established. The trend line grouping brought qualitative picture about the role of substitutions on the mechanical properties which is useful in screening of designed polymers for deemed applications. Comparison of the Poisson's ratio shows that except azetidine side chain polyethers all designed polymers possess superior plastic properties, since they have larger Poisson's ratio (about 0.3). Predicted explosive performance of these polymers revealed that pyrazole derivatives are superior in terms of performance while the triazole and tetrazole derivatives are predicted to exhibit moderate performance.

### Supporting Information

Section 1 contains the details about elastic constants. Section 2 describes the Hoffman's relaxation protocol. Table S1 list the cell relaxation protocol used in the calculations. The glass transition temperature ( $T_g$ ) plots of other designed polymer.

### Author Information

Corresponding Author

\*E-mail: sradha78@yahoo.com

### Acknowledgements

The authors thank Director, HEMRL for his approval to publish this work. The authors acknowledge the support of ACRHEM, University of Hyderabad. The authors also thank G. M. Gore, HEMRL, S. Premkumar, ARDE, Pune and Dr. V. D. Ghule, NIT, Kurukshetra for helpful discussions.

### References

- [1] G.X. Sun, Polymer Blended Explosives, Defense Industry Press, Beijing, 1984.
- [2] H.S. Dong, F.F. Zhou, High Energy Explosives and Correlative Physical Properties, Science Press, Beijing, 1984.
- [3] R.L. Simpson, P.A. Urtiew, D.L. Ornellas, G.L. Moody, K.J. Scribner, D.M. Hoffman, Propell. Explos. Pyrotech. 22 (1997) 249.
- [4] A.H. Ghee, P. Sreekumar, Energetic Polymers, Wiley-VCH, Weinheim, 2012.
- [5] U.R. Nair, S.N. Asthana, A.S. Rao, B.R. Gandhe, Defence Sci. J. 60 (2010) 137.

- [6] D.M. Hoffman, L.E. Caley, Polym. Engi. Sci. 26 (1986) 1489.
- [7] J.F. Geng, Y. L. Lao, J. Beijing Univ. Sci. Tech. (in Chinese) 11 (1991) 87.
- [8] A. Balley, J.M. Bellerby, S.A. Kinloch, Philos. Trans. R. Soc. Lond. 339 (1992) 321.
- [9] W.S. Yao, J.W. Dai, H.M. Tan, Acta Armamentarii (in Chinese) 2 (1994) 11.
- [10] X.Z. Yang, Molecular Simulation and Macromolecule Material, Science Press, Beijing, 2002.
- [11] H.M. Xiao, J.S. Li, H.S. Dong, J. Phys. Org. Chem. 14 (2001) 644.
- [12] D.S. Thomas, M. Ralph, B. Dmitry, D.S. Grant, J. Chem. Phys. 119 (2003) 7417.
- [13] X.J. Xu, H.M. Xiao, J.J. Xiao, W. Zhu, H. Huang, J.S. Li, J. Phys. Chem. B 110 (2006) 7203.
- [14] X. Xu, J.J. Xiao, H. Huang, J. Li, H.M. Xiao, J. Hazard. Mater. 175 (2010) 423.
- [15] J. Xiao, H. Huang, J. Li, H. Zhang, W. Zhu, H.M. Xiao, J. Mol. Struct. (THEOCHEM) 851 (2008) 242.
- [16] L. Qiu, H.M. Xiao, W.H. Zhu, J.J. Xiao, W. Zhu, J. Phys. Chem. B 110 (2006) 10651.
- [17] W.J. Cho, J. Kim, J. Lee, T. Keyes, J.E. Straub, K.S. Kim, Phys. Rev. Lett. 112 (2014) 157802.
- [18] J.R. Errington, J. Chem. Phys. 118 (2003) 9915.
- [19] H.L. Cui, G.F. Ji, X.R. Chen, Q.M. Zhang, D.Q. Wei, F. Zhao, J. Chem. Eng. Data 55 (2010) 3121.
- [20] S. Radhakrishnan, V.D. Ghule, A.K. Sikder, J. Mol. Model. 20 (2014) 2253.
- [21] J.S. Bermejo, C.M. Ugarte, Macromol. Theory Simul. 18 (2009) 259.
- [22] D. Hofmann, L. Fritz, J. Ulbrich, C. Schepers, M. Bohning, Macromol. Theory Simul. 9 (2000) 293.
- [23] N.Ch. Karayiannis, V.G. Mavrantzas, D.N. Theodorou, Macromolecules 37 (2004) 2978.
- [24] D.N. Theodorou, U.W. Suter, Macromolecules 19 (1986) 139.

- [25] U.W. Suter, B.E. Eichinger, *Polymer* 43 (2002) 575.
- [26] J. Xiao, X. Ma, W. Zhu, Y. Huang, H. Xiao, *Propell. Explos. Pyrotech.* 32 (2007) 355.
- [27] L. Qiu, H. Xiao, *J. Hazard. Mater.* 164 (2009) 329.
- [28] M.M. Li, F.S. Li, R.Q. Shen, X. Guo, *J. Hazard. Mater.* 186 (2011) 2031.
- [29] M.M. Li, F.S. Li, R.Q. Shen, *Chin. J. Chem. Phys.* 24 (2011) 199.
- [30] J. Han, R.H. Gee, R.H. Boyd, *Macromolecules* 27 (1994) 7781.
- [31] T. Belytschko, S.P. Xiao, G.C. Schatz, R.S. Ruoff, *Phys. Rev. B* 65 (2002) 1.
- [32] H. Sun, *J. Phys. Chem. B* 102 (1998) 7338.
- [33] C.M. Enrilgo, M. Heuchel, D. Hofmann, A. Lerbret, Y. Yampolskii, *Macromolecules* 36 (2003) 8528.
- [34] M.J. Kamlet, S.J. Jacobs, *J. Chem. Phys.* 48 (1968) 23.
- [35] M.J. Kamlet, J.E. Ablard, *J. Chem. Phys.* 48 (1968) 36.
- [36] P. Politzer, J.S. Murray, *Cent. Eur. J. Energ. Mater.* 8 (2011) 209.
- [37] A. Simperler, A. Kornherr, R. Chopra, P.A. Bonnet, W. Jones, W.D.S. Motherwell, G. Zifferer, *J. Phys. Chem. B* 110 (2006) 19678.
- [38] L.Q. Liao, Y. Zheng, J.Z. Li, *Chin. J. Energ. Mater.* 19 (2011) 113.
- [39] U. R. Nair, S. N. Asthana, A. Subhananda Rao, B. R. Gandhe, *Def. Sci. J.* 60 (2010) 137.
- [40] J.J. Jutier, A.D. Gunzbourg, R.E. Prud'homme, *J. Polymer Sci. Part. A Polymer Chem.* 37 (1999) 1027.
- [41] C. Wu, W. Xu, *Polymer* 47 (2006) 6004.
- [42] S.F. Pugh, *Philos. Mag.* 45 (1954) 823.



### List of Tables

**Table 1.** Molecular formula (M.F.), molecular weight (M.W.), density ( $\rho$ ), heat of formation (HOF), chemical energy of detonation (Q), velocity of detonation (D), and detonation pressure (P) for designed polymers.

Compd.	M.F.*	M.W.	$\rho$ (g/cc)	HOF (kJ/mol)	Q cal/g	D (km/s)	P (GPa)
I1	C <sub>240</sub> H <sub>366</sub> N <sub>60</sub> O <sub>33</sub>	4614	0.979	-39	416.0	3.8	4.0
I2	C <sub>240</sub> H <sub>336</sub> N <sub>90</sub> O <sub>33</sub>	5004	1.203	-89	382.4	4.2	5.9
I3	C <sub>240</sub> H <sub>336</sub> N <sub>90</sub> O <sub>33</sub>	5004	1.202	-61	383.2	4.2	5.9
I4	C <sub>270</sub> H <sub>396</sub> N <sub>90</sub> O <sub>93</sub>	6384	1.221	-127	841.7	5.2	9.2
I5	C <sub>240</sub> H <sub>306</sub> N <sub>120</sub> O <sub>153</sub>	7314	1.220	-84	1210.1	5.6	10.7
P1	C <sub>240</sub> H <sub>366</sub> N <sub>60</sub> O <sub>33</sub>	4614	1.146	7	418.1	4.1	5.5
P2	C <sub>240</sub> H <sub>336</sub> N <sub>90</sub> O <sub>93</sub>	5964	1.267	-39	903.9	5.4	10.2
P3	C <sub>270</sub> H <sub>336</sub> N <sub>60</sub> O <sub>33</sub> F <sub>90</sub>	6654	1.274	-689	1149.2	5.7	11.6
P4	C <sub>300</sub> H <sub>306</sub> N <sub>60</sub> O <sub>33</sub> F <sub>180</sub>	8694	1.377	-1373	1537.3	6.4	15.4

T1	$C_{210}H_{336}N_{90}O_{33}$	4644	1.132	14	416.1	4.3	5.9
T2	$C_{210}H_{336}N_{90}O_{33}$	4644	1.177	91	420.1	4.4	6.4
T3	$C_{210}H_{306}N_{120}O_{93}$	5994	1.293	-3	901.0	5.6	11.2
T4	$C_{180}H_{336}N_{150}O_{33}$	5124	1.278	241	388.4	4.9	8.3
T5	$C_{210}H_{366}N_{120}O_{33}$	5094	1.186	219	389.3	4.5	6.7
A1	$C_{240}H_{456}N_{30}O_{33}$	4284	0.746	-58	446.0	3.4	2.5
A2	$C_{240}H_{396}N_{30}O_{33}F_{60}$	5364	0.642	-491	1068.1	4.0	3.0
NIMMO	$C_{150}H_{276}N_{30}O_{123}$	4464	1.243	-283	1581.5	6.3	13.7
AMMO	$C_{150}H_{276}N_{90}O_{33}$	3864	1.211	135	503.1	4.9	8.2
BAMO	$C_{150}H_{246}N_{180}O_{33}$	5094	1.324	454	396.2	5.0	8.9

\*Cell contains 3 chains that are terminated with hydroxyl group and in each chain 10 monomeric units are present.

**Table 2.** Calculated glass transition temperature data of various designed polymers.

Polymer	T <sub>g</sub> (K)	Polymer	T <sub>g</sub> (K)	Polymer	T <sub>g</sub> (K)	Polymer	T <sub>g</sub> (K)
I1	265	P1	269	T1	216	A1	265
I2	239	P2	283	T2	186	A2	304
I3	270	P3	249	T3	232	NIMMO	239(243)*
I4	204	P4	266	T4	275	AMMO	237(238)*
I5	257			T5	262	BAMO	250(246)*

\*Experimental values

**Table 3.** Calculated mechanical properties of the designed polymers.

Polymer	Modulus (GPa)			Poisson's Ratio ( $\gamma$ )	K/G
	Young's (E)	Bulk (K)	Shear (G)		
I1	7.51	6.38	2.88	0.30	2.22
I2	6.91	5.55	2.67	0.29	2.08
I3	7.94	5.06	3.20	0.24	1.58

I4	4.48	4.45	1.68	0.33	2.65
I5	6.79	5.08	2.66	0.28	1.91
P1	7.66	5.46	3.03	0.27	1.80
P2	6.31	3.13	2.71	0.16	1.15
P3	5.30	4.13	2.06	0.29	2.00
P4	4.72	2.84	1.93	0.22	1.47
T1	4.87	4.68	1.84	0.33	2.55
T2	3.52	3.46	1.32	0.33	2.61
T3	8.59	5.30	3.50	0.23	1.52
T4	4.68	4.76	1.75	0.34	2.72
T5	3.88	3.02	1.51	0.29	2.01
A1	11.66	6.40	4.87	0.20	1.31
A2	6.63	3.80	2.74	0.21	1.39
polyNIMMO	3.01	2.53	1.15	0.30	2.19
polyAMMO	2.10	2.34	0.78	0.35	3.01
polyBAMO	4.01	3.03	1.57	0.28	1.93

**Table 4.** Relative order of susceptibility to deformation in the designed polymers.

Side chain group	Moduli	Poisson's Ratio
Imidazole	I3 > I1 > I2 > I5 > I4	I4 > I1 > I2 > I5 > I3
Pyrazole	P1 > P2 > P3 > P4	P3 > P1 > P4 > P2
Triazole	T3 > T1 > T2	T1 = T2 > T3
Tetrazole	T4 > T5	T4 > T5
Azetidine	A1 > A2	A2 > A1

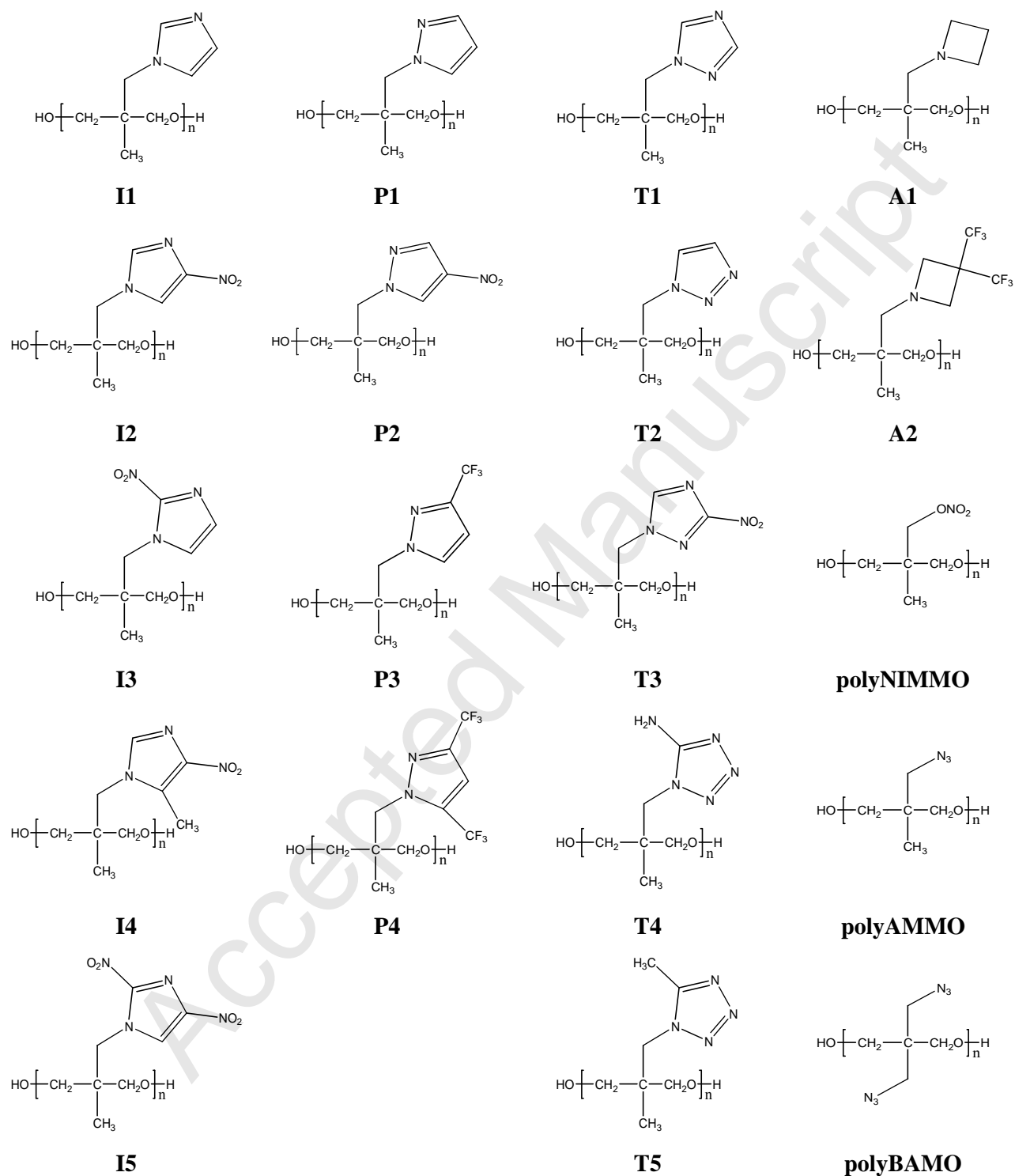


**Fig. 1.** Chemical structures of designed polymers.

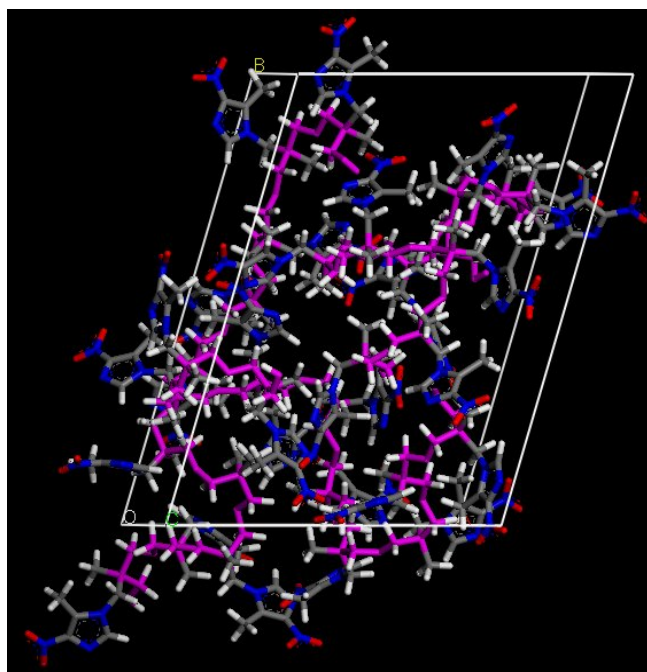


**Fig. 2.** Representative cell of relaxed PolyI4.

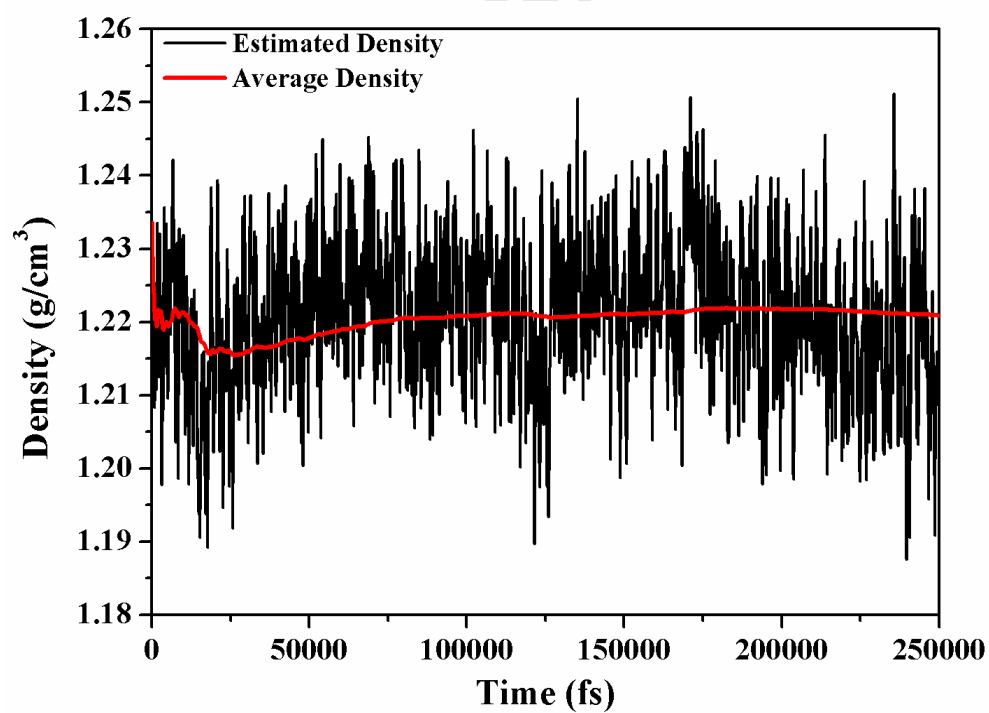


**Fig. 3.** Density variation during NPT dynamics simulations and average density prediction.

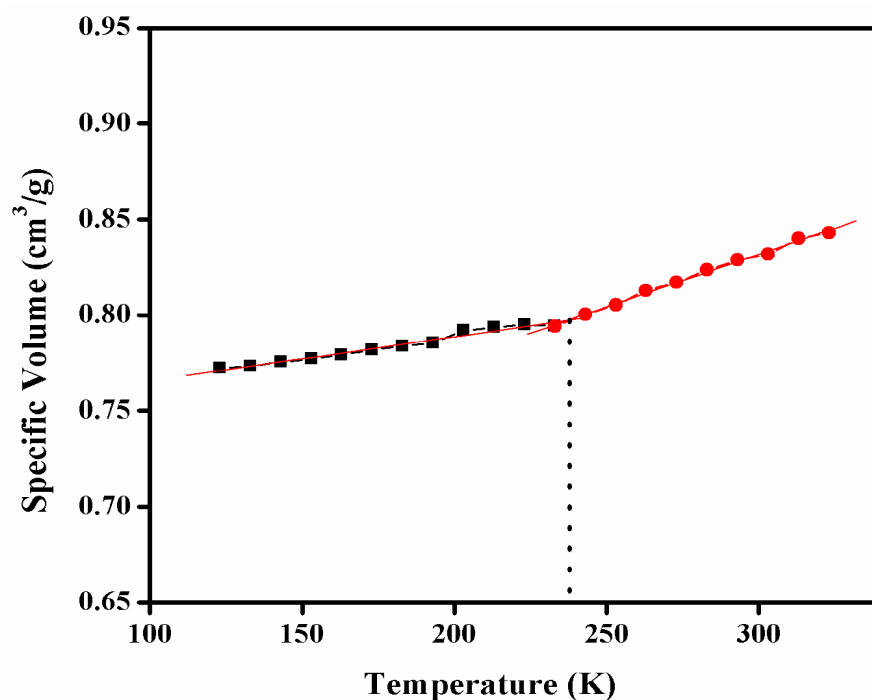


**Fig. 4.** The change of specific volume as a function of temperature of polyAMMO.  
(Intersecting point of fit of two linear regression lines through the data points of glass phase (■) and rubbery phase (●) is noted as  $T_g$ )

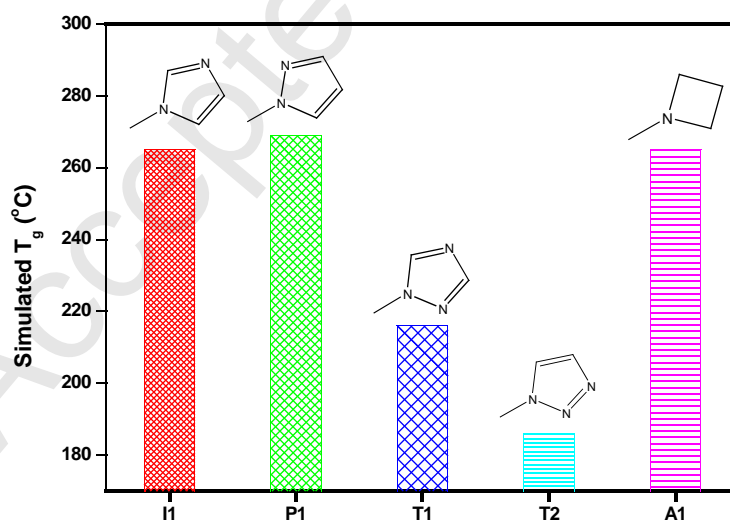


**Fig. 5.** Simulated glass transition temperature of designed polyethers with unsubstituted heterocyclic side chains.

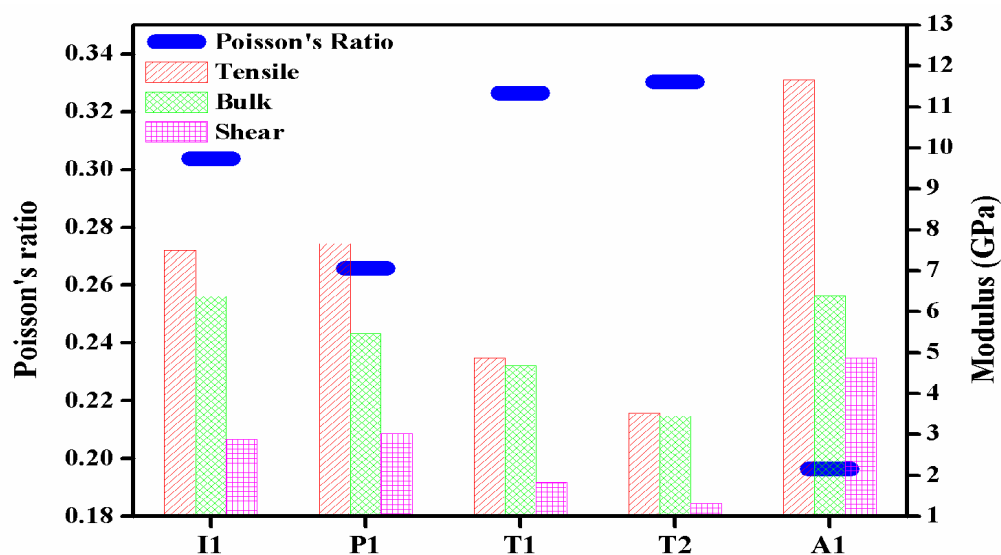


**Fig. 6.** Comparison of modulus data of designed polyethers with unsubstituted heterocyclic side chains.

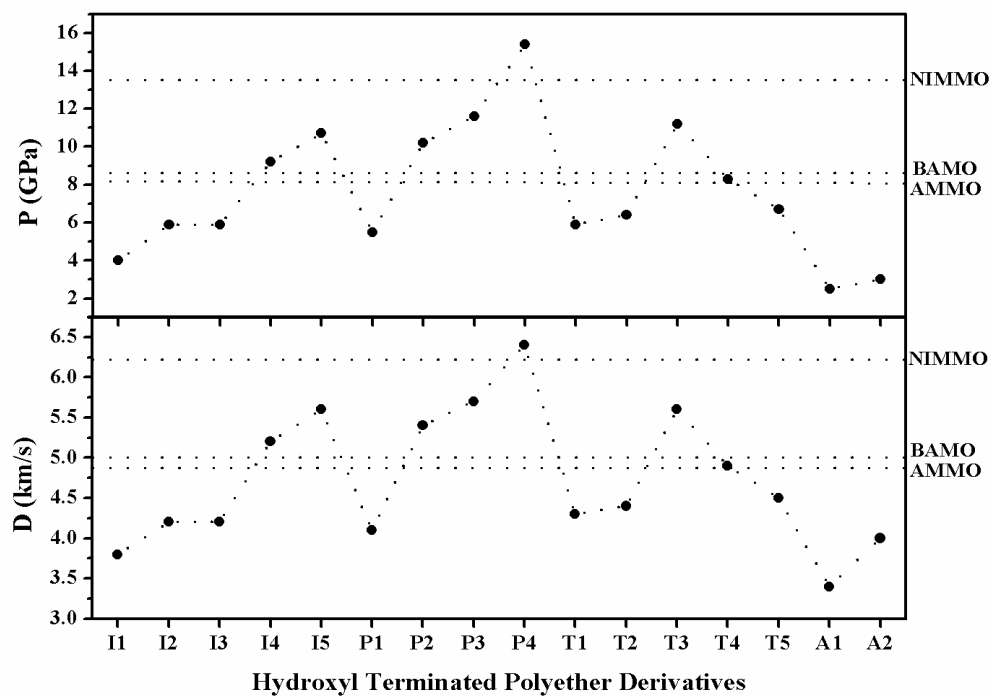


**Fig. 7.** Calculated detonation velocity and pressure data of designed polymers with polyNIMMO, polyAMMO and polyBAMO.